PCCP

Accepted Manuscript

This article can be cited before page numbers have been issued, to do this please use: J. Espinosa-Garcia and C. Rangel, *Phys. Chem. Chem. Phys.*, 2018, DOI: 10.1039/C7CP07592H.

ROYAL SOCIETY OF CHEMISTRY

rsc.li/pccp

View Article Online
DOI: 10.1039/C7CP07592H

Full-dimensional analytical potential energy surface describing the gas-phase Cl + C_2H_6 reaction and kinetics study of rate constants and kinetic isotope effects

Cipriano Rangel and Joaquin Espinosa-Garcia*
Departamento de Química Física and Instituto de Computación Científica Avanzada, Universidad de Extremadura, 06071 Badajoz (Spain)
* Corresponding authors: joaquin@unex.es

Abstract

Within the Born-Oppenheimer approximation a full-dimensional analytical potential energy surface, PES-2017, was developed for the gas-phase hydrogen abstraction reaction between the chlorine atom and ethane, which is a nine bodies system. This surface presents a valence-bond/molecular mechanics functional form dependent on 60 parameters and is fitted to high-level *ab initio* calculations. This reaction presents little exothermicity, -2.30 kcal mol^{-1}, with a low height barrier, 2.44 kcal mol^{-1}, and intermediate complexes in the entrance and exit channels. We found that the energetic description was strongly dependent on the *ab initio* level used and it presented a very flat topology in the entrance channel, which represents a theoretical challenge in the fitting process. In general, PES-2017 reproduces the *ab initio* information used as input, which is merely a test of self-consistency. As a first test of the quality of the PES-2017, a theoretical kinetics study was performed in the temperature range 200-1400 K using two approaches, i.e. variational transition-state theory and quasi-classical trajectory calculations, and with spin-orbit effects. The rate constants show reasonable agreement with experiments in the whole temperature range, with the largest differences at the lowest temperatures, and this behaviour agrees with previous theoretical studies, thus indicating the inherent difficulties in theoretical simulation of the kinetics of the title reaction. Different sources of error were analysed, such as limitations of the PES and theoretical methods, recrossing effects, tunnelling effect, which is negligible in this reaction, and the way in which the spin-orbit effects were included in this non-relativistic study. We found that variation of spin-orbit coupling along the reaction path,

View Article Online
DOI: 10.1039/C7CP07592H

and the influence of the reactivity of the excited $Cl(^2P_{1/2})$ state, have relative importance, but do not explain the whole discrepancy. Finally, the activation energy and the kinetics isotope effects reproduce the experimental information.

View Article Online
DOI: 10.1039/C7CP07592H

TOC

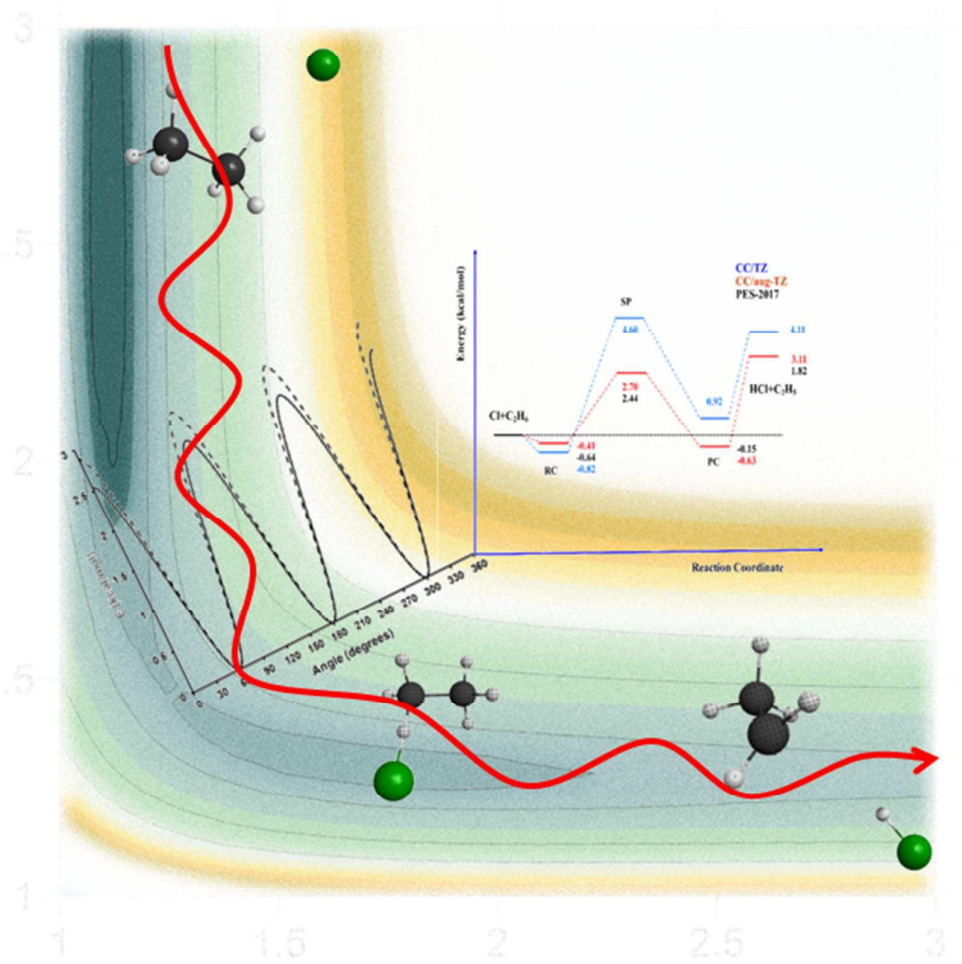

View Article Online
DOI: 10.1039/C7CP07592H

1. Introduction

The construction of potential energy surfaces (PES), together with dynamics methods (classical or quantum), represent the key elements in the theoretical study of chemical reactivity. This process began in a systematic way in the middle of last century with the study of atom-diatom systems, in which the foundations of dynamics understanding of reactivity were established. The step from triatomic to polyatomic systems represented a significant advance in this understanding. In recent decades, practically beginning with the 21st century, a great development has occurred in the study of polyatomic reactions, with the benchmark hydrogen abstraction reaction between hydrogen and methane. Different strategies have been used in the construction of PESs, which describe nuclei motion in the field of the electrons, Born-Oppenheimer approximation. Several research groups have developed surfaces for polyatomic systems (see, for instance, Refs. 1-8 and references therein, although obviously the list is not exhaustive): OH + XH, describing four bodies; X + NH_3, five bodies; X + CH_4, six bodies; or XY + CH_4, seven bodies (where X, Y refer usually to H, O or halogen atoms). Our group in fact constructed the first surface in 1996 for the F + CH_4 reaction,[9] and the last was published in 2017 describing the CN + CH_4 hydrogen abstraction reaction.[10] During this period more than 20 analytical full-dimensional PESs have been constructed for different polyatomic systems, all of which are easily located in the POTLIB library.[11]

A strong test of the quality of the PES is its capacity to simulate experiments, both kinetics and dynamics (although, obviously, in this comparison the theoretical tools must also be taken into account). This theory/experiment comparison has served, firstly, to describe the strengths and weakness of each PES and theoretical method, and secondly, to improve in both directions. The PES describing the seven atom OH + CH_4 reaction, developed by our group in 2015[12], is an analytical global surface based on valence-bond augmented with molecular mechanics (VB-MM) functions and fitted to a reduced and selected number of high-level *ab initio* calculations, and has permitted simulation at a very high level of detail the fine velocity map imaging (VMI) 2005's experiments performed by Kopin Liu[13-15]for this reaction and its isotopic analogues, when a rigorous treatment of the quasi-classical results was performed.[16,17]

View Article Online
DOI: 10.1039/C7CP07592H

The next step in this development was to increase the size of the molecular system, where the construction of the surface for the reaction between hydrogen atom and ethane, nine bodies, by Truhlar et al.[4] represented a pioneering work. Later, Greaves et al.[18] developed a semiempirical PES for the title reaction, using the AM1 semiempirical Hamiltonian specific to this reaction. In the present work we have studied the Cl + C_2H_6 reaction, and using a different methodology have developed for the first time its analytical PES based on *ab initio* data. The abundance of kinetics[19-23]and dynamics[24-28] experimental studies represents a hard test bench to analyze the quality of the new PES. Experimentally this reaction shows high reactivity (for instance, at room temperature, it is faster than the analogue Cl + CH_4 reaction by a factor of ~500) with a low activation barrier, 0.2±0.2[29], and a small dependence on temperature. The latest review[19] reported the following rate constant expression ($cm^3molecule^{-1}s^{-1}$)

$$k(T) = 3.9.10^{-11} (T/298\ K)^{0.70} \exp(0.97(kJ\ mol^{-1})/RT) \quad (1)$$

in the temperature range 203-1400 K. From the dynamics point of view, a controversy about the available energy deposited in the ethyl radical product of the reaction exists amongst different groups,[24,26,28] and in spite of the similarities with the Cl + CH_4 reaction, Suits et al.[28] concluded that its dynamics behaviour is more complicated than could be expected from a simple direct mechanism. This abundance of experimental studies contrasts with the paucity of theoretical works,[18,30-34] where the kinetics is analyzed in Refs. 31-33, and the dynamics in Refs. 18, 33, 34, generally by using low-level computational methods, except in Ref. 18.

The main objective of the present work is the development of an analytical full-dimensional PES describing the nine bodies hydrogen abstraction reaction, Cl + C_2H_6 → HCl + C_2H_5 which, due to the low activation barrier, represents a serious theoretical challenge. With this information, the second objective is to obtain the thermal rate constants and kinetics isotope effects (KIE) at different temperatures, and to compare the results with the available experimental data. This kinetics study will permit us to analyze the role of tunneling and recrossing effects on reactivity. The paper is structured as follows. In Section 2 the high-level *ab initio* calculations used in the fitting of the PES are outlined, with special attention to the intermediate complexes, which have not always been reported and characterized in previous theoretical studies. The functional form and the fitting process of the new PES are developed in detail in Section 3. The kinetics computational details and the kinetics results, rate constants and KIEs, are presented in Sections 4 and 5, respectively, where two very different approaches are

View Article Online
DOI: 10.1039/C7CP07592H

used: variational transition-state theory (VTST) and quasi-classical trajectory (QCT). Finally, Section 6 summarizes the main conclusions.

2. Electronic structure calculations

Previous theoretical studies[18,32,33] showed that the energetic description of this reactive system is strongly dependent on the level of calculation used, and that a very high level is necessary to correctly describe it. For a clearer discussion about the role of the basis set, we present here an analysis by steps, where only at the end it is seen that the experimental measurements are reproduced when very high *ab initio* levels are used. In sum, this represents a didactic presentation, emphasizing the role of the basis set and the computational effort. All *ab initio* calculations were performed by using the Gaussian09 code.[35]

a) We chose as a first approximation to the problem the CCSD(T)=FC/cc-pVTZ *ab initio* level, which represents a compromise between accuracy and computational effort, given the number of points calculated to describe the PES and the molecular size (47 electrons). Thus, all stationary points on the reaction path were optimized and characterized (vibrational frequency) at this level.

We begin by analysing the standard enthalpy of reaction, $\Delta H_r^o(298K)$, which presents small controversies between different experimental sources: -2.67±0.5 kcal mol^{-1} (Ref. 36) and -2.08±0.39 kcal mol^{-1} (Ref. 37). Taking into account these error bars, the experimental results show an uncertainty of ~ ±1 kcal mol^{-1}. The energy of reaction, ΔE_R, obtained at the CCSD(T)=FC/cc-pVTZ level is 4.11 kcal mol^{-1}, and corrected with the zero-point energy (ZPE, 0K) and thermal corrections (TC, 298K), gives a standard enthalpy of reaction of -0.44 kcal mol^{-1}. Note that at this level the spin contamination is negligible, $<S^2>$ close to 0.75. However, this comparison lacks the consideration of spin-orbit (s-o) coupling, which is present in the reactant chlorine but quenched in the products. In our non-relativistic calculations the two electronic states of the chlorine atom, $^2P_{3/2}$ and $^2P_{1/2}$, are degenerate, but in a relativistic study s-o coupling splits them, with a separation from experiment of 882 cm^{-1} (2.5 kcal mol^{-1})[36]. Consequently, the electronic ground-state $^2P_{3/2}$ decreases its energy by one third of its non-relativistic energy, 0.84 kcal mol^{-1}. In non-relativistic calculations, therefore, this effect can be taken into account by adding 0.84 kcal mol^{-1} to the energy of reaction. The standard enthalpy of reaction at 298 K is now +0.40 kcal mol^{-1}, far from the

View Article Online
DOI: 10.1039/C7CP07592H

experimental value, which indicates that higher *ab initio* levels are necessary. Note that in the previous theoretical studies[18,30-34] s-o coupling was not considered.

Next, the possible intermediate complexes in the entrance and exit channels are analysed. In the entrance channel, we found a complex (RC, reactant complex) stabilized 0.82 kcal mol^{-1} with respect to the reactants. When the ZPE correction is included, ΔH (0K) = -2.10 kcal mol^{-1}. In this case s-o coupling is not considered because we calculate that this effect is not quenched in the complex (see below, Section 5.2). In the van der Waals complex the chlorine atom is bonded to two hydrogens on the same carbon atom, with Cl…H distances of 3.076 and 3.064 Å. This RC complex was reported by Rudic et al.[34] and Greaves et al.[18] with a stabilization < 1 kcal mol^{-1}, and a Cl…H distance of 2.7 Å. The complex in the exit channel (PC, product complex) is destabilized +0.92 kcal mol^{-1} with respect to the reactants, but stabilized -3.19 kcal mol^{-1} with respect to the products. It presents a C…H' bond of 2.128 Å, close to the value reported by Fernandez-Ramos et al.,[33] 2.078 Å, and the value given by Greaves et al.,[18] 2.06 Å, using lower *ab initio* levels. When the ZPE correction is included the PC is stabilized by -1.63 kcal mol^{-1} with respect to the products (note that with respect to the products, s-o coupling is not considered because it is quenched in the PC complex and in the products).

Finally, we analyse the saddle point, which is characterized by one and only one imaginary frequency. The formed (Cl…H') and broken (H'…C) bonds show values, respectively, of 1.472 and 1.364 Å, with an imaginary frequency of 968i cm^{-1}, and a classical barrier height of $\Delta E^{\neq}$ = 4.60 kcal mol^{-1}. The geometry and imaginary frequency agree with previous results,[18,32-34] where the formed bond is larger than the broken one (values between 1.46 and 1.50 Å and between 1.31 and 1.37 Å, respectively, were reported depending on the level used), and the imaginary frequencies reported are 831 and 900 i cm^{-1}. The largest difference is found in the barrier height, with reported values from -1.07 to +4.1 kcal mol^{-1}.

In order to check reliability of the electronic structure calculations (mainly the role of the basis set) we used two previous sets of data (Table 1). The first was reported by Greaves et al.[18] for the title reaction, where basis sets from double-zeta to quadruple-zeta were analysed. These show that the increase of the basis set decreases the barrier height, from 4.15 to 2.20 kcal mol^{-1}. The s-o correction was not included in the original paper, but when we included it, a best estimate of 2.37 kcal mol^{-1} was obtained, intermediate between the aug-cc-pVTZ and the aug-cc-pVQZ values without s-o

View Article Online
DOI: 10.1039/C7CP07592H

corrections. The second set of data was reported by Czako and Bowman[38] for the similar Cl + CH_4 reaction, where larger basis sets (up to 6-zeta) were analysed (Table 1). The role of the basis set is similar to the previous results, decreasing the barrier height from 9.65 kcal mol^{-1} with the triple-zeta basis set to 6.84 kcal mol^{-1} with the aug-cc-pV6Z. When s-o coupling is included (which these authors assume quenched in the saddle point) the best estimate is 7.71 kcal mol^{-1}, close to the value obtained with the aug-cc-pVTZ basis set without s-o corrections. Therefore, the aug-cc-pVTZ basis set seems to compensate two opposite errors: basis set and s-o coupling. These results reveal that the barrier height is strongly dependent on the basis set, and that these calculations are unapproachable with our computational resources.

b) Based on this information and in order to improve the energetic description of the title system, we increase the basis set by using the single-point method: CCSD(T)=FC/aug-cc-pVTZ//CCSD(T)=FC/cc-pVTZ, where the energy is calculated at the higher level on the optimized geometries at the lower level. Firstly, the classical reaction energy decreases from 4.11 to 3.11 kcal mol^{-1}, and taking into account the ZPE and s-o corrections it gives a standard enthalpy of reaction of -0.64 kcal mol^{-1}. Exothermicity of the reaction is now well reproduced, although it is still far from the experimental data. Secondly, the increase of the basis set has little effect on the stabilization of the intermediate complexes. The RC therefore slightly reduces stability with respect to the reactants, $\Delta H^o(0K)$ = -1.70 kcal mol^{-1}, and the PC increases it slightly with respect to the products, $\Delta H^o(0K)$ = -3.74 kcal mol^{-1}. Finally, we observe that the largest effect is on barrier height, which diminishes from 4.60 to 2.70 kcal mol^{-1}. As a consequence of this lower barrier, imaginary frequency diminishes, significantly lower than 968 i cm^{-1}. Therefore, we conclude that the effect of the basis set on the energetic description of this reactive system is very great, and possibly higher computational levels than the one used here, CCSD(T)=FC/aug-cc-pVTZ//CCSD(T)=FC/cc-pVTZ single-point level, are necessary for an accurate description.

c) In fact, we follow increasing the basis set, and now we use the very expensive (for our computational resources) aug-cc-pV5Z basis set, and the coupled-cluster method, CCSD(T)=FC/aug-cc-pV5Z single-point level. Now ΔE_R = 1.73 kcal mol^{-1}, ΔH^o_R (298 K)= -2.69 kcal mol^{-1}, reproducing one experimental value,[36] and when the s-o correction is included in the *ab initio* calculations, ΔE_R = 2.57 kcal mol^{-1}, ΔH^o_R (298 K)= -1.85

View Article Online
DOI: 10.1039/C7CP07592H

kcal mol^{-1}, thus reproducing the other experimental value.[37] The barrier height is $\Delta E^{\neq}$ = 1.87 kcal mol^{-1}, or 2.71 kcal mol^{-1} if the s-o correction is included. Note that this s-o corrected barrier is similar to that obtained with the lower CCSD(T)=FC/aug-cc-pVTZ level without s-o effects, a fact which is merely due to an error cancelation, as was shown in previous calculations (Table 1) by analysing the Cl + CH_4 and Cl + C_2H_6 reactions.

We summarize the basis set effect in Figure 1, where the energetic profile of the reaction is shown for the most significant stationary points. This flat reaction path and the presence of intermediate complexes represent a theoretical challenge in the development of an analytical full-dimensional PES for this hydrogen abstraction reaction.

3. Potential energy surface: functional form and fitting process

Our research group has developed analytical global surfaces for reactive systems of five (X + NH_3 type), six (X + YH_4 type) or seven (XZ + YH_4 type) bodies, where X,Y, Z = F, Cl, Br, H, C, Si, Ge, N. Theoretical kinetics and dynamics studies were performed based on these surfaces, obtaining in all cases a qualitative, and even on occasions a quantitative, agreement with the experimental data available. The natural step in this evolution was the development of surfaces for larger systems. In the present work we present the results for the nine bodies system, Cl + C_2H_6 → HCl + C_2H_5, which opens the door to kinetics and dynamics studies of larger compounds at a relatively low computational cost compared to the considerably higher costs if high-level *ab initio* calculations are performed to describe the whole system, which are usually thousands of calculations.

Based on our experience in this field, the PES was constructed in a two-step process: first, the analytical functional form was developed as a valence bond (VB) function augmented with molecular mechanics (MM) terms, in brief, VB/MM, which depends on adjustable parameters. These were then fitted to the previous *ab initio* calculations. A term-by-term description of all terms in the PES and the fitting process are provided as **Supplementary Information**, a brief summary only being provided here for the purposes of understanding the remainder of the paper.

a) Analytical functional form. To maintain the potential physically intuitive, in relation with chemical concepts, the potential energy, V, of the whole system is

View Article Online
DOI: 10.1039/C7CP07592H

expressed as the sum of stretching V_{str} describing the C-H_i bonds, stretching V_{CC} describing the C-C bond, bending $V_{bending}$, out-of-plane bending V_{op} and torsional V_{tor} terms:

$$V = V_{str} + V_{CC} + V_{bending} + V_{op} + V_{tor} \quad (2)$$

V_{str} is developed as the sum of six LEP (London-Eyring-Polanyi) stretching terms describing the six C-H bonds, and it depends on 26 parameters,

$$V_{\text{stret}} = \sum_{i=1}^{6} V_3\left(R_{\text{CH}_i}, R_{\text{CCl}}, R_{\text{H}_i\text{Cl}}\right) \quad (3)$$

V_{CC} is represented by a Morse function describing the C-C bond, depending on 3 adjustable parameters,

$$V_{CC} = D_{CC}^{1}[1 - \exp\{-\alpha_{CC}(R_{CC} - R_{CC}^{o})\}]^2 \quad (4)$$

$V_{bending}$ represents the bending motions of the reactive system, based on harmonic potentials with respect to the reference angles in ethane, θ^{o}_{ij}, and the corresponding force constants, k_i, and depends on 22 parameters,

$$V_{bending} = \frac{1}{2}\sum_{i=1}^{5}\sum_{j=i+1}^{6} k_{ij}^{0} k_i k_j \left(\theta_{ij} - \theta_{ij}^{0}\right)^2 \quad (5)$$

The out-of-plane motions are represented by the potential V_{op}, which is a quadratic-quartic potential, in function of the respective force constants $f_{\Delta i}$ and $h_{\Delta i}$, depending on 6 parameters,

$$V_{\text{op}} = \sum_{i=1}^{6} f_{\Delta_i} \sum_{\substack{j=1 \\ j\neq i}}^{6} \left(\Delta_{ij}\right)^2 + \sum_{i=1}^{6} h_{\Delta_i} \sum_{\substack{j=1 \\ j\neq i}}^{6} \left(\Delta_{ij}\right)^4 \quad (6)$$

where the angle Δ_{ij} measures the deviation from the reference angle θ^{o}_{ij},

$$\Delta_{ij} = acos\left(\frac{(\vec{q_k}-\vec{q_j})\times(\vec{q_l}-\vec{q_j})}{\|(\vec{q_k}-\vec{q_j})\times(\vec{q_l}-\vec{q_j})\|} \cdot \frac{\vec{r}_i}{||\vec{r}_i||}\right) - \theta_{ij}^{0} \quad (7)$$

with $(q_k\text{-}q_j)$ and $(q_l\text{-}q_j)$ being two vectors between three hydrogens on each carbon and r_i the vector between the carbon and each of the hydrogens directly bonded to it. Finally, the torsion motion about the C-C bond, V_{tor}, is represented by,

$$V_{tor} = \sum_{i=1}^{3}\sum_{l=1}^{3} \frac{v_3}{3}(1 + \cos\gamma)\,.T(w_1, w_2) \quad (8)$$

where v_3 is the torsional barrier height, γ the torsional angle and $T(w_1,w_2)$ a switching function depending on two parameters. Total, 3 adjustable parameters.

View Article Online
DOI: 10.1039/C7CP07592H

Finally, note that numerous switching functions are included in the terms of Eq. (2) to permit smooth changes from reactants to products while the reaction evolves; these are hyperbolic tangent functions permitting smooth changes in the process.

In total, the new PES depends on 60 parameters. Note that compared with the previously developed similar and smaller system, Cl + CH_4 reaction[39], the number of fitting parameter increases from 33 to 60, which represents a severe difficulty in the fitting process.

b) Fitting process. The second step in the development of the PES is the fitting of the 60 parameters to the high-level *ab initio* calculations used as input. In total, about 44 000 ab initio points were calculated describing, mainly, the minimum energy path and the reaction valley. By using the least-squares method, fitting is a four-step iterative process. First, the reactant and product properties (geometry, energy and vibrational frequencies) are fitted to the *ab initio* data. Next, the saddle point properties (especially barrier height) are fitted, taking into account the ambiguities in the *ab initio* information, even when using very high *ab initio* methods, and in the s-o corrections. These factors actually introduce uncertainties of ~ 1 kcal mol^{-1}, which are too great given the sensitivity of the description of this reactive zone. Thus, specifically, we used the s-o corrected classical barrier obtained at the highest *ab initio* level available, 2.71 kcal mol^{-1}, as an upper limit (Section 2). The iterative fitting procedure of the PES, gives a barrier height of 2.44 kcal mol^{-1}, reproducing the *ab initio* input data. Third, the *ab initio* information describing the intermediate complexes in the entrance and exit channels is used to fit the properties of these stationary points. This step proved to be especially hard in the entrance channel, because of the very flat topology in this reactant zone and the low stability of the RC. Finally, the minimum energy path, MEP, and the reaction valley (which includes the orthogonal vibrational motions to the MEP) are fitted to the *ab initio* data. This four-step process is tedious, because it must be repeated until convergence is reached with the *ab initio* information used as input data. Once the fitting process was concluded, we obtained the final set of 60 parameters defining the new PES-2017 surface.

Note, however, that different strategies in the development of PESs for polyatomic systems have been used by different groups.[1-8] For instance, for the oxygen + ethylene reaction, Bowman and coworkers[40] used the permutationally invariant polynomial method fitted to high level *ab initio* calculations at the RCCSD(T)/AVTZ level, to describe the singlet and triplet surfaces.

View Article Online
DOI: 10.1039/C7CP07592H

4. Kinetics computational details

Using two approaches, variational transition-state theory (VTST) and quasi-classical trajectory (QCT) calculations, the thermal rate constants were calculated on the PES-2017 surface, at temperatures in the range 200-1400 K, and were compared with the available theoretical and experimental data.

a) VTST approach. Using the microcanonical version of this theory,[41,42] μVT, the thermal rate constants are given by

$$k^{\mu VT}(T) = \sigma \frac{k_B T}{h} K^o \exp\left[-\Delta G(T, s^{*,\mu VT}) / k_B T\right] \quad (9)$$

where σ is the symmetry factor (6 for the forward reaction), k_B is the Boltzmann constant, K^o is the reciprocal of the standard-state concentration, 1 molecule cm^3, and $\Delta G(T,s^{*,\mu VT})$ represents the maximum of the free energy of activation along the reaction coordinate, s. For the chlorine electronic partition function, the two electronic states, $^2P_{3/2}$ and $^2P_{1/2}$ (ε = 882 cm^{-1}) are taken into account,[36] while the spin-orbit coupling in the saddle point is assumed to be fully quenched. Hence the following total electronic partition function ratio is used in Eq.(9),

$$f = \frac{2}{4 + 2\exp(-\varepsilon / k_B T)} \quad (10)$$

This multisurface temperature factor accounts for the fraction of reactants colliding on the ground-state PES. Note that this coefficient diminishes the theoretical rate constants by a factor of about two over the whole temperature range. This point will be analyzed later. While the rotational partition functions were calculated classically, the vibrational modes are treated as separable harmonic oscillators using redundant internal coordinates,[43-45] with the exception of the lowest vibrational mode, in which anharmonicity is included by using the hindered rotor model (RW model).[46]

A priori tunnelling should play a significant role at low temperatures, given the heavy-light-heavy mass combination; however, given that this reaction presents a low barrier height, with a negative adiabatic barrier (see Fig. 1), this effect is negligible. In the VTST theory the rate constant is obtained by varying the dividing surface between reactants and products at a point s*(T) where the ΔG(T,s*) is maximum and consequently the rate constant is minimum. The separation between this s* point and

View Article Online
DOI: 10.1039/C7CP07592H

the saddle point, defined at s = 0, is named variational effect. All kinetics calculations were performed using the POLYRATE-2016 program.[47]

b) QCT approach. At each temperature, 100 000 trajectories were run with an initial and final C-Cl separation of 15.0 Å, sufficient to ensure that no interaction is present in the reactant and product asymptotes, with a propagation step of 0.1 fs. Reactant rotational and vibrational energies were chosen by thermal sampling at each temperature. The maximum impact parameter, b_{max}, varies little with temperature, from 6.4 Å at 200 K to 6.3 Å at 1400 K. These values at each temperature were obtained by calculating batches of 5 000 trajectories at fixed values of b, increasing this value until no reactive trajectories were found. The reaction cross section is given by

$$\sigma_r(T) = \pi b_{\max}{}^2 \frac{N_r}{N_T} \tag{11}$$

where the Monte Carlo sampling of the initial conditions is used, and N_r y N_T are, respectively, the reactive and total number of trajectories at each temperature. The estimated error is

$$\Delta\sigma_r(T) = \sigma_r(T)\sqrt{\frac{N_T - N_r}{N_T . N_r}} \tag{12}$$

and given the number of trajectories run, the maximum error is <5%. Finally, the thermal rate constant is given by

$$k(T) = f.\left(\frac{8k_B T}{\pi\mu}\right)^{1/2} \sigma_r(T) \tag{13}$$

where μ is the reduced mass. Since the QCT calculations are classical in nature they do not include quantum effects, such as tunneling or spin-orbit effect. In this case, tunneling is negligible, and s-o coupling is included by a multiple-surface coefficient, f (Eq. 10).

For temperatures in the range 200-1400 K, QCT calculations were carried out using standard procedures implemented in the VENUS program,[48,49] adapted to incorporate the new analytical PES.

5. Results and discussion

View Article Online
DOI: 10.1039/C7CP07592H

5.1 Comparison with *ab initio* calculations. In order to test the quality of the PES-2017 we compare its results against the *ab initio* data used as input in the fitting process for all stationary points in the path

$$Cl + C_2H_6 \rightarrow RC \rightarrow SP \rightarrow PC \rightarrow HCl + C_2H_5$$

Tables 2 and 3 show the geometry, vibrational frequency and energy of the stationary points along the reaction path. The geometry of reactants and products (Table 2) is well reproduced, while the vibrational frequencies also show good agreement taking into account that the *ab initio* calculations overestimate the vibrational frequencies. In fact, in all stationary points we observed a linear regression between PES and *ab initio* vibratioanl frequencies with $R^2 \geq 0.99$ (see Tables 2 and 3). As was previously noted, the energy of reaction is strongly dependent on the level of calculation, and so the value obtained with PES-2017 reproduces the energy using the highest level, CCSD(T)=FC/aug-cc-pV5Z. Taking into account the previous considerations, overestimation of the *ab initio* vibrational frequencies and strong dependence of the relative energies, PES-2017 also reasonably reproduces the other stationary points (SP, RC and PC, Table 3). The largest differences being the broken C..H´ bond in the saddle point, error of 0.1 Å, and the Cl …H´ bond in the reactant complex, error of 0.7 Å. We suppose that these differences will not affect the final kinetics results. Thus the barrier height, 2.44 kcal mol^{-1}, is close to the *ab initio* information when the s-o correction is included, 2.71 kcal mol^{-1}, where the largest difference corresponds to the imaginary frequency, 732 i cm^{-1} versus 968 i cm^{-1}. However, it must be remembered that the 968 i cm^{-1} value corresponds to the imaginary frequency obtained at the CCSD(T)=FC/cc-pVTZ *ab initio* level, which presents a barrier height of 4.60 kcal mol^{-1}. Therefore, if the barrier height lowers with the basis set, cc-pVTZ → aug-cc-pVTZ → aug-cc-pV5Z, the imaginary frequency will also lower. This behaviour agrees with the value 732 i cm^{-1} obtained with the PES-2017 surface.

Next, the torsional potentials for ethane and saddle point are presented in Figure 2 by using PES-2017 and CCSD(T)=FC/aug-cc-pVTZ for comparison. Ethane shows a three-fold rotation profile, i.e., it presents three maxima (and three minima) on rotating 360º about the C-C bond. The torsional barrier height with PES-2017 is 2.54 kcal mol^{-1}, close to the *ab initio* value, 2.91 kcal mol^{-1}, and to the experimental ones, 2.88 kcal mol^{-1} (Ref. 50). The internal rotational motion of the methyl group in the ethyl radical is practically free, with low barrier height, 0.38 kcal mol^{-1} at the CCSD(T)=FC/aug-cc-pVTZ level, in agreement with the PES-2017 value, 0.65 kcal mol^{-1}. Finally, we analyse

View Article Online
DOI: 10.1039/C7CP07592H

this motion at the saddle point. The barrier heights show good agreement, 1.67 and 1.98 kcal mol^{-1} using PES-2017 and *ab initio* level. Note that in all cases, the PES-2017/*ab initio* barrier height difference is <0.5 kcal mol^{-1}, which confirms the accuracy of the functional form and the fitting process describing this sensitive internal motion.

Finally, the bending motion of the saddle point is analysed. The correlation between the diatomic rovibrational distribution and the bending motion of the saddle point (Cl…H'…C) is well known. Schatz et al. in atom-diatom[51] and polyatomic[52] systems reported that different rotational distributions in the products can be obtained in PESs with the same saddle point but with different dependency of the energy on the bending motion. They concluded, therefore, that hotter rotations are related with looser saddle points. In addition, in previous works on the similar $Cl + CH_4 \rightarrow HCl + CH_3$ reaction we also showed this correlation,[39,53] where the cold HCl rotational distribution was explained by the repulsive character of the bending motion, i.e., tighter saddle point. For the title reaction, Figure 3 presents this energy dependence of the Cl …H'…C bending angle of the saddle point for PES-2017 and CCSD(T)=FC/aug-cc-pVTZ *ab initio* level for comparison. Both curves show good agreement, the largest difference (7 kcal mol^{-1}) being obtained when the separation from linearity is 60º. Given that both curves are repulsive, a rotational cold HCl product is expected. This behaviour will be analysed in future dynamics calculations.

In sum, given the large number of degrees of freedom (21) involved in this polyatomic system (9 bodies), PES-2017 reasonably reproduces the whole *ab initio* information used as input, in stationary points, reaction path, reaction valley and zones far from the reaction path, although in this case this latter information is less important since the tunnelling effect is small or negligible (see below).

5.2. Rate constant calculations. Table 4 and Figure 4 present the theoretical rate constants (μVT and QCT) using the PES-2017 surface in the temperature range 200-1400 K, together with the experimental values[19] for comparison. The conventional transition-state theory values (where the transition state is located at the saddle point, s* = 0), TST, are also included for posterior analysis. Both μVT and QCT methods present similar behaviour, and in general they reproduce the experimental data over the whole temperature range, with errors between 60 and 10% for the μVT method and between 53 and 24% for the QCT approach, the largest differences being at the lowest

View Article Online
DOI: 10.1039/C7CP07592H

temperatures. To go further into this analysis we studied the low and high temperature regimes separately. In the low temperature regime the differences with the experiment are more important. A priori, given the heavy-light-heavy mass combination present in the reaction, tunnelling should play an important role, but in this case where the adiabatic barrier is below the adiabatic reactant asymptote this effect is negligible. So by using semiclassical expressions, such as small (SCT) or large (LCT) curvature tunnelling methods[54] the tunnelling factor is the unity in the whole temperature range. However, when the simple unidimensional Wigner expression[55] is used, which takes into account the classical minimum energy path and the imaginary frequency at the saddle point, the rate constants are multiplied by factors between 2.14 at 200 K and 1.02 at 1400 K, thus approaching the theoretical values to the experiment. Obviously, this very simple method is a rather naive approach to the problem, but it does show that small variations in the reaction path in the proximity of the transition state zone (as analysed in Section 2, on the role of the basis set) may vary the role of tunnelling in this reaction at low temperatures. As the temperature increases the errors decrease, and so at 1400 K the errors are 10 and 24 % for the μVT and QCT methods, respectively. This agreement with the experiment (taking into account the experimental uncertainties) seems to show that the barrier height, 2.44 kcal mol^{-1}, obtained with PES-2017, correctly describes the reactive system.

Note that previous theoretical rate constant calculations have also been marked by difficulties (see Fig. 4). Roberto-Neto et al.[31,32] in the temperature range 250-1000 K found that the theory differs from the experiment by a factor ~2.5, the difference being larger (by a factor ~4) at the lower temperatures. Fernandez-Ramos et al.[33] reported good theory/experiment agreement in the temperature range 200-500 K, but at higher temperatures the theory overestimates the experiment by a factor ~2. Note that this agreement can be fortuitous because these authors did not consider the s-o effects. In sum, these theoretical results show the difficulties in obtaining an accurate description of the kinetics of the title reaction, related with difficulties in the accurate description of the barrier height and the very flat topology in the entrance channel, all of which represent an authentic theoretical challenge.

The present theoretical results also show these difficulties, underestimating the experimental values, and in order to analyse the possible reasons, several sources of error were checked (note that although they are analysed individually, some of these issues can be related):

View Article Online
DOI: 10.1039/C7CP07592H

a) Limitations of the theoretical tools, PES and dynamics method (μVT and QCT). When one compares theory with experiment, both the dynamics method and the PES are tested. Obviously, the initial focus in the search is related with deficiencies in the PES. As was previously described (Section 2), the fitting process uses exclusively high level *ab initio* information, and this input data is reasonably reproduced by the PES, where the most characteristic points (reactants, products, saddle point, intermediate complexes with the corresponding vibrational frequencies, or reaction path and reaction swatch) are reasonably reproduced. Therefore, the possible limitations of the PES are related with the difficulties in the accurate description of this reactive system by using *ab initio* calculations, and their limitations in the level used. The second focus is related with the dynamics method (μVT and QCT). The rate constants in the wide temperature range 200-1400 K obtained with both methods show good agreement, with the largest difference being 17%. As both theories use the same surface, the very different theoretical approaches are not responsible for the theory/experiment differences.

b) Recrossing effects. The title reaction is a good candidate to present large recrossing effects, given that it is an almost thermoneutral reaction and presents a heavy-light-heavy mass combination.[41,42,56] This effect is also known as "variational effect" and measures the displacement of the maximum ΔG(T) from the saddle point (s* = 0). It is computed as the ratio between the variational and conventional transition state results, μVT/TST. From columns 2 and 3 of Table 4, the recrossing effects on the rate constants are very important, varying from 0.016 at 200 K to 0.310 at 1400 K. In all cases the generalized transition state, s*(T), is located in the entrance channel, with values from s* = -0.413 a_o at 200 K to s* = -0.241 a_o at 1400 K. In the VTST theory this effect is minimized by varying the dividing surface between reactants and products to maximize ΔG(T) and to minimize the rate constant. However, the location of the generalized transition state dividing surface is strongly dependent on the reaction path (which is very flat in the entrance channel) and the variation of the vibrational frequencies (especially the lowest ones) on the reaction path. Small variations of the dividing surface can cause significant changes in the rate constants, especially at the lower temperatures, where the recrossing effects are more important. Therefore, in the study of the recrossing effects we are assessing the validity of the VTST approach and the quality of the PES, because both issues are related.

View Article Online
DOI: 10.1039/C7CP07592H

c) Anharmonic treatment of the vibrational frequencies. This issue is closely related with the previous one, because the location of the dividing surface (one of the weakest points of the VTST theory) depends on the vibrational modes of lowest frequency and their variation along the reaction path. These low values are related with large vibrational partition functions and small $\Delta G(T)$. Therefore, accurate anharmonicity treatment is crucial in the correct description of the dividing surface and finally of the rate constants. In the present work, anharmonicity of the lowest mode was considered by using the hindered rotor model (Section 4a), while the remaining modes were considered as harmonic.

To estimate the influence of these related effects, recrossing/anharmonicity, on the rate constants, the QCT calculations can be of great utility because they are independent of the location of the dividing surface. In general, both theories, VTST and QCT, show good agreement, with the largest difference, 17%, occurring at the lowest temperature. As both theories use the same PES-2017 surface, we conclude that the approaches included in the VTST theory have a small influence on the final results (or alternatively their effects are compensated). In a previous study on the Cl + CH_4 reaction[39] we found similar and important recrossing effects, varying from 0.027 at 200 K, with $s^* = -0.455\ a_o$ to 0.206 at 1000 K, with $s^* = -0.443\ a_o$. However, in this case, in spite of these large variational effects, the influence on the final rate constants was negligible, or alternatively, they were compensated with other effects, such as tunnelling at low temperature, which are important for this system, contributing with factors from 16.73 to 1.24 in the 200-1000 K temperature range. Therefore, a priori these effects are not principally responsible for the discrepancies with the experiment.

d) Spin-orbit effects. The chlorine atom presents two spin-orbit electronic states, $^2P_{3/2}$ and $^2P_{1/2}$, which are split by $\varepsilon = 882\ cm^{-1}$ (2.5 kcal mol^{-1})[36], and it is usually assumed that this coupling is quenched as the reaction progress. In non-relativistic calculations (such as the present one) this s-o coupling effect is taken into account in two ways: on the barrier height and on the electronic partition function, Q_e. As was analysed in Section 2, the first effect is to increase the barrier height. So in order to incorporate s-o coupling in non-relativistic rate constant calculations, i.e., to simulate the s-o effect, it is necessary to lower the energy of the chlorine reactant by $1/3\varepsilon$ (0.84 kcal mol^{-1}), which is

View Article Online
DOI: 10.1039/C7CP07592H

equivalent to increasing the barrier height by this amount. The second effect is on Q_e. $Q_e(Cl)$ takes the conventional temperature dependence expression, considering the degeneracy,

$$Q_e(Cl) = 4 + 2\exp(-\frac{\epsilon}{k_B T}) \quad (10)$$

where the s-o ground-state of Cl, $^2P_{3/2}$, is taken as reference. However, it is usually assumed that $Q_e(TS) = 2$ along the reaction path, i.e., as the reaction evolves s-o coupling decreases practically to zero, and so it is practically quenched in the transition state zone. This variation in s-o interaction and its effect on the kinetics of the reaction has been rarely studied.[57-60] In general, these few studies conclude that if the separation of the fragments in the transition state zone is small it is assumed that the s-o effect is quenched in this zone, $Q_e(TS) = 2$, whereas if the separation is large then s-o splitting is close to its asymptotic fragments and its variation is negligible, $Q_e(TS) \sim Q_e(Cl)$. Obviously these are two limits to the problem and all intermediate situations can be present. For instance, Parker et al.[58] analyzing the $Cl + CH_3$ reaction found that the rate constants are strongly dependent on the s-o variation, which yields uncertainties of a factor greater than 2 in the final rate constants.

A rigorous analysis of the s-o variation requires relativistic calculations, which are very complex in polyatomic systems and are beyond the scope of the present work. As a first approximation to the problem, we calculated this s-o variation as the reaction evolves based on CASSCF/aug-cc-pVDZ calculations with five electrons and three orbitals, using the MOLPRO code.[61] Taking as reference the experimental s-o coupling of the chlorine atom,[36] which is one-third of the s-o splitting, i.e., 1/3 ε = 294 cm^{-1}, we obtained a value of 273 cm^{-1}, in close agreement with the experiment. As a test of quality of the method used, the s-o splitting of the Cl atom was also computed with the cc-pVTZ basis set with a larger active space, five electrons in six orbitals, with similar results. Thus, we use the cheaper method in the next discussion. Geometry dependence of s-o coupling at different points of the reaction path are listed in Table 5. It is well known that s-o coupling is largely dominated by single-center terms, so it is reasonable to scale these facts up by a geometry-independent constant. Therefore we scaled all these results up by an empirical correction factor of 1.077 (i.e. the ratio between the experimental and the calculated s-o splitting: 294/273 = 1.077, or 7.7 %). These scaled values also appear in Table 5, and they are shown in Figure 5. It may be observed that the s-o coupling lowers as the reaction evolves, 214 cm^{-1} for the reactant complex, 19.0

View Article Online
DOI: 10.1039/C7CP07592H

cm^{-1} for the transition state (s* = -0.4121 a_o) and 8.5 cm^{-1} for the saddle point (s* = 0). These results show that quenching is small in the reactant complex, is practically total at the saddle point, and is again small but not negligible at the transition state. Although this is a first approximation to the problem, note that previous theoretical studies did not consider this effect. Jasper et al.[60] proposed an empirical factor correction, C, to include s-o effects in non-relativistic calculations,

$$k"_{so}(T) = k(T)\exp(-\frac{C\varepsilon}{3k_BT}) \qquad (14)$$

where k(T) and k"$_{so}$(T) are, respectively, the non-relativistic and corrected rate constants, and the temperature dependent C factor is given by

$$C(T) = 1 - \frac{E_{so}[s*_{\mu VT}(T)]}{\varepsilon_{/3}} \qquad (15)$$

where $E_{so}[s*_{\mu VT}(T)]$ is the s-o coupling value at $s*_{\mu VT}(T)$. Given that in this reaction the transition state zone scarcely varies with temperature, from -0.413 to -0.241 a_o in the whole temperature range 200-1400 K, and that s-o coupling is small in this zone (Table 5), the factor C ~0.93-0.97. This indicates that the corrected rate constants (k"$_{so}$) are larger than the non-relativistic values (k) by factors between15% at 200 K and 2% at 1400 K. In sum, in the absence of more accurate relativistic calculations, we estimate the influence of this s-o coupling factor to be small, 15%, although not negligible, especially at lower temperatures.

e) Reactivity of the excited Cl($^2P_{1/2}$) state. In general, the experimental kinetics studies for the chlorine atom do not differentiate between the reactivity of the two electronic states, Cl($^2P_{3/2}$) and Cl($^2P_{1/2}$). For the atom-diatom Cl(^2P) + H_2 reaction numerous studies, both theoretical and experimental, have been reported (see for instance, Refs, 62-66 and references therein), and theory/experiment controversies exist about the role of the excited Cl($^2P_{1/2}$) s-o state in reactivity. In general, the ratio Cl($^2P_{1/2}$)/ Cl($^2P_{3/2}$) reactivity changes with the collision energy, where the reactivity of the Cl($^2P_{1/2}$) state is negligible at high energies but significant at lower collision energies. For the reaction with methane,

Cl(^2P) + CH_4, experimental studies show no evidence of a contribution to reaction from Cl($^2P_{1/2}$).[67-69] For the title reaction, however, Hitsuda et al.[70,71] experimentally reported that the rate coefficient at room temperature for the Cl($^2P_{1/2}$) + C_2H_6 reaction was $<3.10^{-11}$ cm^3 $molecule^{-1}$ s^{-1}; i.e., only about 2-fold slower than the corresponding reaction for the electronic ground-state reaction, Cl($^2P_{3/2}$) + C_2H_6. If s-o excitation were

View Article Online
DOI: 10.1039/C7CP07592H

effective to overcome the barrier one would expect the opposite behaviour. These authors suggested that the nonadiabatic pathway of $Cl(^2P_{1/2}) + C_2H_6 \rightarrow HCl + C_2H_5$ is still effective although should be small under the experimental conditions.

This tendency in the series, $Cl(^2P) + CH_4$, $Cl(^2P) + H_2$ and $Cl(^2P) + C_2H_6$, is related with the barrier height, 7.6, 5.7 and 2.4 kcal mol^{-1}, respectively. Thus, the possible nonadiabatic pathway from the $Cl(^2P_{1/2})$ reaction (although small) should increase the probability of reaction and the rate constant, this being easier the lower the barrier is. In sum, the role of the s-o excited state, $Cl(^2P_{1/2})$ in the reactivity depends on the reaction, and even so, it is an open question.

These ambiguities (incorporation of s-o effects in non-relativistic studies, the role of the s-o coupling variation as the reaction evolves, and the role of the excited $Cl(^2P_{1/2})$ state) create uncertainties in kinetics studies of the chlorine atom, and therefore the relative theory/experiment agreement (better at higher temperatures) reached in the present work for the title reaction seems reasonable.

5.3. Activation energy. To provide a more appropriate comparison with the experiment, the phenomenological activation energy (obtained from the slopes of the Arrhenius plots) at room temperature was computed using VTST and QCT methods. We obtained values of 0.28 and 0.21 kcal mol^{-1}, respectively, in excellent agreement with the experimental value 0.2 ±0.2 kcal mol^{-1}.[29]

Finally, we performed an additional test of quality on the PES-2017, by calculating the standard enthalpy of reaction at 298 K from the activation energies for the forward and reverse reaction using the μVT theory, which are 0.28 and 2.79 kcal mol^{-1}, respectively. With these values $\Delta H^o_r(298K)$ = -2.51 kcal mol^{-1}, which reproduces the experimental data:[36,37] -2.67 ± 0.5 and -2.08 ± 0.39 kcal mol^{-1}. This result shows the balance of the forward and reverse reactions and confirms the characteristics and quality of the potential energy surface developed for this system.

5.4. Kinetics isotope effects (KIEs). The H/D and $^{12}C/^{13}C$ KIEs are important because they are used to elucidate the sources of hydrocarbons and as reference reactions in relative kinetics studies. They are defined in the conventional way, i.e., as the ratio of the rate constants for the lighter to the heavier system, and they are less dependent on the accuracy of the PES. For H/D KIE, i.e., $Cl + C_2H_6$/ $Cl + C_2D_6$, the only reported experimental value is at room temperature, with the most recent KIE of 3.1 reported by Hitsuda et al.[70] although values in the range 2.69-5.80 have been reported.[72-76] The

View Article Online
DOI: 10.1039/C7CP07592H

calculated VTST and QCT KIEs at 298 K on the same PES-2017 surface are 3.4 and 3.0, respectively, which are in agreement between themselves and reproduce the most recent experiment. These results show that both theoretical methods are adequate to study the kinetics of this reaction.

As for the $^{12}C/^{13}C$ KIE, it is of special importance in Titan atmosphere because it permits us to know its origin and evolution.[77] The $^{12}C/^{13}C$ KIEs obtained with the μVT/PES-2017 method are 1.018 at 175 K (to simulate the Titan atmosphere) and 1.025 at 298 K (to simulate the Earth's atmosphere). The former value has been not experimentally measured, but this very low value agrees with the hypothesis raised by Jennings et al.[77] to explain the Titan atmosphere. Basically, they assume that ethane in Titan derives from atmospheric methane, via methyl radicals, and the $^{12}C/^{13}C$ KIE in ethane is similar to the $^{12}C/^{13}C$ ratio in methane. The latter value reproduces the findings by Anderson et al.,[78] 1.011 at 298 K, although it is slightly overestimated. Finally, the $^{12}C/^{13}C$ KIEs for the title reaction, Cl + C_2H_6, are lower than those obtained for the similar reaction with methane (298 K), 1.067 obtained by our group using the VTST theory,[39] which agrees with the experiments, in the range 1.058-1.066.[79-82] This methane/ethane tendency concurs with the experimental evidence.[82]

6. Conclusions

Using high-level *ab initio* data characterizing the most important zones of the Cl + C_2H_6 hydrogen abstraction reaction, we developed its analytical full-dimensional potential energy surface, PES-2017, which is a combination of valence-bond and molecular mechanics terms related with the internal motions of the reactive system.

In the first test, the accuracy of the new PES-2017 was analysed by comparison with the *ab initio* data used in the fitting, which is a test of self-consistency. This surface correctly describes the exothermicity of the reaction, $\Delta H^o_r(298K)$ = -2.30 kcal mol^{-1}, as compared with the experimental values, -2.67 ± 0.5 and -2.08 ± 0.39 kcal mol^{-1}; the barrier height, 2.44 kcal mol^{-1}, as compared with recent and accurate estimates, 2.37 kcal mol^{-1}, and very high-level *ab initio* calculations, 2.71 kcal mol^{-1}, and the very flat topology in the entrance channel, which represented a challenge in this development. In addition, the surface correctly describes intermediate complexes in the entrance and exit channels, with stabilities similar to previous theoretical studies. From this analysis of the *ab initio* information used as input, we conclude that the topology of

View Article Online
DOI: 10.1039/C7CP07592H

the title reaction is very sensitive to the level of calculation, which complicates the theoretical study.

Using the VTST and QCT theories on this PES-2017 we compared the kinetics information obtained with experimental data, thus performing a second test of quality. First, both theories agree between themselves in the whole temperature range, 200-1400 K, with differences <17%, indicating that both theories are adequate to study the kinetics of this reaction, which is reasonable because the tunnelling effect is negligible in this case. Second, both theoretical rate constants show reasonable agreement with experiments at high temperatures, which shows that the barrier height is well described, but they underestimate the experimental values, ~50%, at the lower temperatures. Possible sources of error were analysed, such as limitations of the theoretical tools (PES and dynamics method), or the importance of the recrossing effects, concluding that their influence on the final results is small. In addition, the effect of s-o coupling (and its variation along the reaction path), and the influence of the reactivity of the excited $Cl(^2P_{1/2})$ state, which were not considered in previous theoretical studies, seem to influence the kinetics of the reaction. However, the quantitative participation of these issues are today an open question, because they require accurate relativistic calculations and breakdown of the Born-Oppenheimer approximation, which are beyond the scope of the present work.

In sum, within the Born-Oppenheimer approximation, i.e., using only the electronic ground-state, where the s-o effects are included *ad hoc*, the PES-2017 describes the topology of the title reaction from reactants to products and reports a kinetics study in reasonable agreement with the experiment. These results lend confidence to the quality of the PES for this polyatomic system, and give us hope for future dynamics analyses.

Acknowledgments

This work was partially supported by Gobierno de Extremadura, Spain (Project No. GR15015). We thank Jose C. Corchado for computational support. The collaborations of Donald G. Truhlar, Minnesota University, USA, and Xuefei Xu, Tsinghua University, China, are appreciated. We thank X. Xu the calculations at the CASSCF level to analyse the s-o effects.

View Article Online
DOI: 10.1039/C7CP07592H

References

1. T. Joseph, R. Steckler and D.G. Truhlar, *J.Chem.Phys.,* 1987, **87**, 7036.
2. M.J.T. Jordan and R.G. Gilbert, *J.Chem.Phys.,* 1995, **102**, 5669.
3. G.E. Moyano and M.A. Collins, *Theor.Chem.Acc*. 2005, **113**, 225.
4. A. Chakraborty, Y. Zhao, H. Lin and D.G. Truhlar, *J.Chem.Phys.,* 2006, **124**, 044315.
5. J.M. Bowman, G. Czako and B. Fu, *Phys.Chem.Chem.Phys*., 2011, **13**, 8094.
6. J. Li, B. Jiang and H. Guo, *J.Chem.Phys.,* 2013, **139**, 204103.
7. G. Czako and J.M. Bowman, *J. Phys. Chem. A,* 2014, **118**, 2839.
8. J. Palma and U. Manthe, *J. Phys. Chem. A,* 2015, **119**, 12209.
9. J.C. Corchado and J. Espinosa-Garcia, *J.Chem.Phys.,* 1996, **105**, 3160.
10. J. Espinosa-Garcia, C. Rangel and Y. Suleimanov, *Phys.Chem.Chem.Phys*., 2017, **19**, 1934.
11. R. J. Duchovic, Y. L. Volobuev, G. C. Lynch, A. W. Jasper, D. G. Truhlar, T. C. Allison, A. F. Wagner, B. C. Garrett, J. Espinosa-Garcia, and J. C. Corchado, POTLIB, http://comp.chem.umn.edu/potlib.
12. J. Espinosa-Garcia and J.C. Corchado, *Theor. Chem. Acc*., 2015, **134**, 6.
13. B. Zhang, W. Shiu, J.J. Lin and K. Liu, *J. Chem. Phys.,* 2005, **122**, 131102.
14. B. Zhang, W. Shiu, J.J. Lin and K. Liu, *J. Phys. Chem. A,* 2005, **109**, 8983.
15. B. Zhang, W. Shiu, J.J. Lin and K. Liu, *J. Phys. Chem. A,* 2005, **109**, 8989.
16. L. Bonnet, J.C. Corchado and J. Espinosa-Garcia, *Comp. Rendue Chem.,* 2016, **19**, 571.
17. L. Bonnet and J. Espinosa-Garcia, *Phys.Chem.Chem.Phys.,* 2017, **19**, 20267.
18. S.T. Greaves, A.J. Orr-Ewing and D. Troya, *J.Phys.Chem. A*, 2008, **112**, 9387.
19. M.G. Bryukov, I.R. Slagle and V.D. Knyazev, *J.Phys.Chem. A*, 2003, **107**, 6565; which is a review of the literature until 2003.
20. K.M. Hickson and L.F. Keiser, *J.Phys.Chem. A*, 2004, **108**, 1150.
21. D.L. Donohoue, D. Bauer and A.J. Hynes, *J.Phys.Chem. A*, 2005, **109**, 7732.
22. N. Choi, M.J. Pilling, P.W. Seakins and L. Wang, *Phys.Chem.Chem.Phys.,* 2006, **8**, 2172.
23. K.M. Hickson, A. Bergeat and M. Costes, *J.Phys.Chem. A*, 2010, **114**, 3038.

View Article Online
DOI: 10.1039/C7CP07592H

24. S. A. Kandel, T.P. Rakitzis, T. Lev-on and R.N. Zare, *J.Chem.Phys.,* 1996, **105**, 7550.
25. S. A. Kandel, T.P. Rakitzis, T. Lev-on and R.N. Zare, *J.Phys.Chem. A,* 1998, **102**, 2270.
26. M.J. Bass, M. Brouard, C. Vallance, T.N. Kitsopoulos, P.C. Samartzis and R.L. Tromes, *J.Chem.Phys.,* 2003, **119**, 7168.
27. W. Li, C. Huang, M. Patel, D. Wilson and A.G. Suits, *J.Chem.Phys.,* 2006, **124**, 011102.
28. C. Huang, W. Li and A.G. Suits, *J.Chem.Phys*., 2006, **125**, 133107.
29. R. Atkinson, D.L. Baulch, R.A. Cox, R.F. Hampson, J.A. Kerr and J. Troe, *J.Phys.Chem. Reference Data*, 1992, **121**, 1125.
30. A. Bottoni and G. Poggi, *J.Mol.Struct. (Theochem),* 1995, **33**, 161.
31. O. Roberto-Neto and F.B.C. Machado, *Theor.Chem.Acc.,* 2001, **107**, 15.
32. O. Roberto-Neto and F.B.C. Machado, *J.Mol.Struct. (Theochem)*, 2002, **580**, 161.
33. A. Fernandez-Ramos, E. Martinez-Nuñez, J.M.C. Marques and S.A. Vazquez, *J.Chem.Phys.,* 2003, **118**, 6280.
34. S. Rudic, C. Murray, J.N. Harvey and A.J. Orr-Ewing, *J.Chem.Phys*., 2004, **120**, 186.
35. M. J. Frisch, et al., Gaussian 09, Revision A1, Gaussian Inc., Wallinford, CT, 2009.
36. JANAF Thermochemical Tables, ed. M. W. Chase, Jr., C. A. Davies, J. R. Downey, D. J. Frurip, R. A. McDonald and A. N. Syverud, National Bureau of Standards, Washington, D.C., 3rd edn, 1985, vol. 14.
37. R. Atkinson, D. L. Baulch, R. A. Cox, J. N. Crowley, R.F. Hampson Jr, J. A. Kerr, M. J. Rossi, and J. Troe, Summary of evaluated kinetic and photochemical data for atmospheric chemistry. Web version: http://www.iupac-kinetic.ch.cam.ac.uk/ (2003).
38. G. Czako and J.M. Bowman, *Science*, 2011, **334**, 343.
39. C. Rangel, M. Navarrete, J.C. Corchado and J. Espinosa-Garcia, *J.Chem.Phys.*, 2006, **124**, 124306.
40. N. Balucani, F. Leonori, P, Casacecchia, B. Fu and J.M. Bowman, *J. Phys. Chem. A* 2015, **119**, 12498.
41. B.C. Garrett, and D.G. Truhlar, *J. Am. Chem. Soc.,* 1979, **101**, 4534.

View Article Online
DOI: 10.1039/C7CP07592H

42. D.G. Truhlar, A.D. Isaacson, and B.C. Garrett, Generalized Transition State Theory, in *The Theory of Chemical Reactions*, edited by M. Baer, CRC, Boca Raton, FL, 1985, Vol. **4.**
43. C.F. Jackels, Z. Gu, and D.G. Truhlar, *J. Chem. Phys.,* 1995, **102**, 3188.
44. G.A. Natanson, B.C. Garrett, T.N. Truong, T. Joseph, and D.G. Truhlar, *J. Chem. Phys.* 1991, **94**, 7875.
45. Y.Y. Chuang, and D.G. Truhlar, *J. Phys. Chem. A* 1997, **101**, 3808.
46. D.G. Truhlar, *J. Comput. Chem.* 1991, **12,** 266.
47. J. Zheng, J.L. Bao, R. Meana-Paneda, S. Zhang, B.J. Lynch, J.C. Corchado,Y.Y. Chuang, P.L. Fast, W.P. Hu, Y.P. Liu, G.C. Lynch, K.A. Nguyen, C.F. Jackles, A. Fernandez-Ramos, B.A. Ellingson, V.S. Melissas, J. Villa, I. Rossi, E.L. Coitiño, J. Pu, T.V. Albu, A. Ratkiewicz, R. Steckler, B. C. Garret, A.D. Isaacson and D.G. Truhlar, POLYRATE-2016-2A, University of Minnesota, Minneapolis, MN, 2016.
48. X. Hu, W.L. Hase and T. Pirraglia*, J.Comp.Chem*. 1991, **12**, 1014.
49. W.L. Hase, R.J. Duchovic, X. Hu, A. Komornicki, K.F. Lim, D-h. Lu, G.H. Peslherbe, K.N. Swamy, S.R. Vande Linde, A.J.C. Varandas, H. Wang, and R.J. Wolf, VENUS96: A General Chemical Dynamics Computer Program, QCPE Bull. 1996, **16**, 43.
50. N. L. Allinger, Y. H. Yuh, and J.-H. Lii, *J. Am. Chem. Soc.,* 1989, **111**, 8551.
51. G. C. Schatz, B. Amaee, and J. N. L. Connor, *J. Chem. Phys.,* 1990, **92**, 4893.
52. D. Troya, R. Z. Pascual, and G. C. Schatz, *J. Phys. Chem. A,* 2003, **107**, 10497.
53. J.C. Corchado, D.G. Truhlar and J. Espinosa-Garcia, *J.Chem.Phys.,* 2000, **112**, 9375.
54. Y-P. Liu, D.h. Lu, A. Gonzalez-Lafont, D.G. Truhlar and B.C. Garrett, *J.Am.Chem.Soc*., 1993, **115**, 7806.
55. E.P. Wigner, *Z.Phys.Chem. Abt. B*, 1932, **19**, 203.
56. D.G. Truhlar, A.F. Wagner and T.H. Dunning, *J.Chem.Phys.,* 1983, **78**, 4400.
57. M. Tashiro and R. Schinke, *J.Chem.Phys.,* 2003, **119**, 10186.
58. J.K. Parker, W.A. Payne, R.J. Cody, F.L. Nesbitt, L.J. Stief, S.J. Klippenstein and L.B. Harding, *J.Phys.Chem.,* 2007, **111**, 1015.
59. A.W. Jasper, S.J. Klippenstein and L.B. Harding, *J.Phys.Chem.,* 2007, **111**, 3932.

View Article Online
DOI: 10.1039/C7CP07592H

60. A.W. Jasper, S.J. Klippenstein and L.B. Harding, *J.Phys.Chem.,* 2010, 114, 5759.
61. H.-J. Werner, P. J. Knowles, G. Knizia, F. R. Manby, M. Schütz, P. Celani, W. Györffy, D. Kats, T. Korona, R. Lindh, A. Mitrushenkov, G. Rauhut, K. R. Shamasundar, T. B. Adler, R. D. Amos, A. Bernhardsson, A. Berning, D. L. Cooper, M. J. O. Deegan, A. J. Dobbyn, F. Eckert, E. Goll, C. Hampel, A. Hesselmann, G. Hetzer, T. Hrenar, G. Jansen, C. Köppl, Y. Liu, A. W. Lloyd, R. A. Mata, A. J. May, S. J. McNicholas, W. Meyer, M. E. Mura, A. Nicklaß, D. P. O'Neill, P. Palmieri, D. Peng, K. Pflüger, R. Pitzer, M. Reiher, T. Shiozaki, H. Stoll, A. J. Stone, R. Tarroni, T. Thorsteinsson and M. Wang; Molpro version 2015, a package of *ab initio* programs; http://www.molpro.net
62. J.M. Bowman, *Science*, 2008, **319**, 40.
63. E. Garand, J.Zhou, D.E. Manolopoulos, M.H. Alexander and D.M. Neumark, *Science*, 2008, **319**, 72.
64. X. Wang, W. Dong, Ch. Xiao, L. Che, Z. Ren, D. Dai, X. Wang, P. Casavecchia, X. Yang, B. Jiang, D. Xie, Z. Sun, S-Y. Lee, D. H. Zhang, H.-J. Werner and M. H. Alexander, *Science,* 2008, **322**, 573.
65. F. Dong, S.H. Lee and K. Liu, *J.Chem.Phys*., 2001, **115**, 1197.
66. M.H. Alexander, G. Capecchi and H.-J. Werner, *Science*, 2002, **296**, 715.
67. J. Zhou, J.J. Lin, B. Zhang and K. Liu, *J.Phys.Chem. A*, 2004, **108**, 7832.
68. Z.H. Kim, A.J. Alexander, H.A. Bechtel and R.N. Zare, *J.Chem.Phys*., 2001, **115**, 179.
69. C. Murray and A.J. Orr-Ewing, *Int.Rev.Phys.Chem.,* 2004, **23**, 435.
70. K. Hitsuda, K. Takahashi, Y. Matsumi and T.J. Wallington, *J.Phys.Chem. A*, 2001, **105**, 5131.
71. K. Hitsuda, K. Takahashi, Y. Matsumi and T.J. Wallington, *Chem.Phys.Lett.*, 2001, **346**, 16.
72. CRC Handbook of Biomolecular and Thermolecular Gas Reactions, edited by J. A. Kerr and S. J. Moss, CRC, Boca Raton, FL, 1981.
73. G. Chiltz, R. Eckling, P. Goldfinger, G. Huybrechts, H. S. Johnston, L. Meyers, and G. Verbeke, *J. Chem. Phys.*, 1963, **38**, 1053.
74. E. Tschuikow-Roux, J. Niedzielski, and F. Faraji, *Can. J. Chem*., 1985, **63**, 1093.
75. S. S. Parmar and S. W. Benson, *J. Am. Chem. Soc.*, 1989, **111**, 57.

View Article Online
DOI: 10.1039/C7CP07592H

76. O. Dobis, S. W. Benson, and T. J. Mitchell, *J. Phys. Chem*., 1994, **98**, 12284.

77. D. E. Jennings, P. N. Romani, G. L. Bjoraker, P. V. Sada, C. A. Nixon, A. W. Lunsford, R.J. Boyle, B. E. Hesman and H. McCabe, *J. Phys. Chem. A,* 2009, **113**, 11101.

78. R. S. Anderson, L. Huang, R. Iannone and J. Rudolph, *J. Phys. Chem. A,* 2007, **111**, 495.

79. G. Saueressig, P. Bergamaschi, J. N. Crowley, H. Fisher and G. W. Harris, *Geophys. Res. Lett.,* 1995, **22**, 1225.

80. J. N. Crowley, G. Saueressig, P. Bergamaschi, H. Fisher and G. W. Harris, *Chem. Phys. Lett.,* 1999, **303**, 268.

81. K. L. Feilberg, D. W. T. Griffith, M. S. Johnson and C. J. Nielsen, *Int. J. Chem. Kinet*., 2005, **37**, 110.

82. S. C. Tyler, H. O. Ajie, A. L. Rice, R. J. Cicerone and E. C. Tuazon, *Geophys. Res. Lett.,* 2000, **27**, 1715.

View Article Online
DOI: 10.1039/C7CP07592H

Table 1. Basis set effect on the classical barrier height (kcal mol^{-1})

Basis set	$Cl + C_2H_6$[a]	$Cl + CH_4$[b]
cc-pVTZ	-	9.65
aug-cc-pVDZ	4.15	7.85
aug-cc-pVTZ	3.12	7.64
aug-cc-pVQZ	2.20	7.06
aug-cc-pV5Z	-	6.81
aug-cc-pV6Z	-	6.84
CBS[c]	1.53	6.87
Best estimate[d]	2.37	7.71

a) Level of calculation: CCSD(T)/basis set//MP2-aug-cc-pVTZ. Ref. 18

b) Level of calculation: CCSDT(Q)/basis set. Ref. 38

c) Complete basis set

d) Including s-o coupling, 0.84 kcal mol^{-1}, to the CBS barrier.

View Article Online
DOI: 10.1039/C7CP07592H

Table 2. Reactants and products properties (distances in Å, frequencies in cm^{-1}, energy in kcal mol^{-1}) with PES-2017 and *ab initio* calculations.

Property	C_2H_6		C_2H_5		HCl	
	PES-2017	*Ab initio*	PES-2017	*Ab initio*	PES-2017	*Ab initio*
C-(H_3)	1.090	1.092	1.092	1.094		
C-(H_2)			1.082	1.081		
Cl-H					1.270	1.277
Frequency[a]						
	2971	3121	3072	3261	2991	3000
	2971	3121	3061	3158		
	2952	3098	3008	3089		
	2952	3098	3008	3063		
	2948	3040	2901	3011		
	2933	3040	1521	1494		
	1542	1512	1521	1491		
	1542	1512	1411	1480		
	1522	1511	1291	1403		
	1522	1511	1067	1200		
	1429	1427	938	1070		
	1394	1406	924	984		
	1173	1224	667	810		
	1010	1224	429	466		
	1010	1015	229	118		
	824	820				
	824	820				
	291	307				
Energy						
ΔE_R[b]	1.82	4.11(3.11)[1.73]				

a) Linear regression between PES and *ab initio* vibrational frequencies:
C_2H_6: $f_{PES} = 0.9495\ f_{ab\ initio} + 38.303$, $R^2 = 0.995$;
C_2H_5: $f_{PES} = 0.9692\ f_{ab\ initio} - 16.447$, $R^2 = 0.995$

b) First value at the CCSD(T)=FC/cc-pVTZ level, in parenthesis at the CCSD(T)=FC/aug-cc-pVTZ single-point level, and in brackets at the CCSD(T)=FC/aug-cc-pV5Z single-point level. No s-o corrections are included.

View Article Online
DOI: 10.1039/C7CP07592H

Table 3. Other stationary point properties (distances in Å, frequencies in cm^{-1}, energy in kcal mol^{-1}) with PES-2017 and *ab initio* calculations.

Property	SP		RC		PC	
	PES-2017	*Ab initio*	PES-2017	*Ab initio*	PES-2017	*Ab initio*
C-H	1.090	1.092	1.089	1.092	1.092	1.094
C-H'	1.244	1.364	1.092	1.093	2.054	2.139
Cl-H'	1.489	1.472	2.584	3.308	1.279	1.291
Frequency[a]						
	2959	3197	2967	3120	3044	3247
	2957	3114	2965	3117	3006	3144
	2939	3110	2946	3096	3000	3096
	2917	3102	2946	3091	2990	3073
	2910	3035	2938	3041	2903	3015
	1510	1500	2914	3033	2886	2782
	1503	1484	1529	1514	1518	1494
	1456	1478	1529	1512	1518	1487
	1398	1406	1497	1509	1485	1479
	1230	1227	1432	1508	1405	1403
	1086	1223	1405	1424	1190	1207
	1063	1076	1336	1404	1012	1067
	998	996	1122	1224	924	993
	956	978	1006	1022	830	812
	825	815	989	1013	513	595
	820	803	822	820	252	381
	505	475	805	818	237	373
	436	416	297	313	228	213
	150	160	74	61	117	110
	137	121	52	49	65	59
	732 i	968 i	31	33	44	44
Energy						
ΔE[b]	2.44	4.60(2.70)[1.87]	-0.64	-0.82(-0.41)	-1.97[c]	-3.19(-2.74)[c]

a) Linear regression between PES and *ab initio* vibrational frequencies:

SP: $f_{PES} = 0.9349\ f_{ab\ initio} + 38.170$, $R^2 = 0.996$;

RC: $f_{PES} = 0.9513\ f_{ab\ initio} + 22.549$, $R^2 = 0.999$;

PC: $f_{PES} = 0.9784\ f_{ab\ initio} - 12.227$, $R^2 = 0.996$.

b) Fist value at the CCSD(T)=FC/cc-pVTZ level, in parenthesis at the CCSD(T)/aug-cc-pVTZ single-point level and in brackets at the CCSD(T)/aug-cc-pV5Z single-point level. The *ab initio* calculations do not include s-o corrections.

c) With respect to the products.

View Article Online
DOI: 10.1039/C7CP07592H

Table 4. Forward rate constants ($cm^3molecule^{-1}s^{-1}$) using PES-2017

T(K)	TST[a]	μVT[b]	QCT[c]	Exp.[d]
200	1.33E-09	2.20E-11	2.52E-11	5.31E-11
300	3.60E-10	2.41E-11	2.90E-11	5.79E-11
400	2.22E-10	2.84E-11	3.30E-11	6.42E-11
500	1.86E-10	3.38E-11	3.69E-11	7.08E-11
600	1.80E-10	4.02E-11	4.25E-11	7.74E-11
700	1.87E-10	4.72E-11	4.80E-11	8.38E-11
800	2.01E-10	5.52E-11	5.40E-11	9.01E-11
1000	2.43E-10	7.33E-11	6.70E-11	1.02E-10
1400	3.64E-10	1.13E-10	9.49E-11	1.25E-10

a) Conventional transition state theory, where the transition state coincides with the saddle point.

b) Microcanonical variational transition state theory, where the transition state is displaced in the reactant channel

c) Quasi-classical trajectory calculations

d) Experimental values from Ref. 19, which is a review of the literature until 2003

View Article Online
DOI: 10.1039/C7CP07592H

Table 5. Spin-orbit coupling (cm^{-1}) along the reaction path for the Cl + C_2H_6 reaction.

System	R(Cl…H')	s*	s-o coupling	s-o scaled[b]
Cl	∞		273	294
RC	2.584		199	214
Point#1	1.776	-1.209	24.5	26.4
Point#2	1.739	-1.000	21.5	23.2
Point#3	1.704	-0.812	19	20.5
TS[a]	1.682	-0.412	17.6	19.0
SP	1.489	0.0	7.9	8.5

a) TS at 300 K
b) s-o coupling scaled by the factor 1.077 (see text).

View Article Online
DOI: 10.1039/C7CP07592H

FIGURE CAPTION

Figure 1. Schematic energy diagram for the Cl + C_2H_6 gas-phase reaction showing the basis set effect. For the PES-2017 surface, the zero-point energy corrected values appear in parenthesis.

Figure 2. Torsional barrier (kcal mol^{-1}) of the ethane (upper panel) and saddle point (lower panel) using PES-2017 (solid line) and CCSD(T)=FC/aug-cc-pVTZ level (dashed line).

Figure 3. Variation of the energy with the bending motion of the saddle point (Cl…H'…C) for the Cl + C_2H_6 reaction, taking as reference the equilibrium geometry, 180º. PES-2017 (solid line) and CCSD(T)=FC/aug-cc-pVTZ level (dashed line).

Figure 4. Arrhenius plot of the thermal forward rate constants vs the inverse of the temperature, comparing the results from the PES-2017 surface with experimental measures from Ref. 19, and previous theoretical studies.[31,33]

Figure 5. Variation of the spin-orbit coupling (cm^{-1}) along the reaction path. The smooth line is used as a guide to the eye, because only seven points were calculated (Table 5).

View Article Online
DOI: 10.1039/C7CP07592H

Figure 1

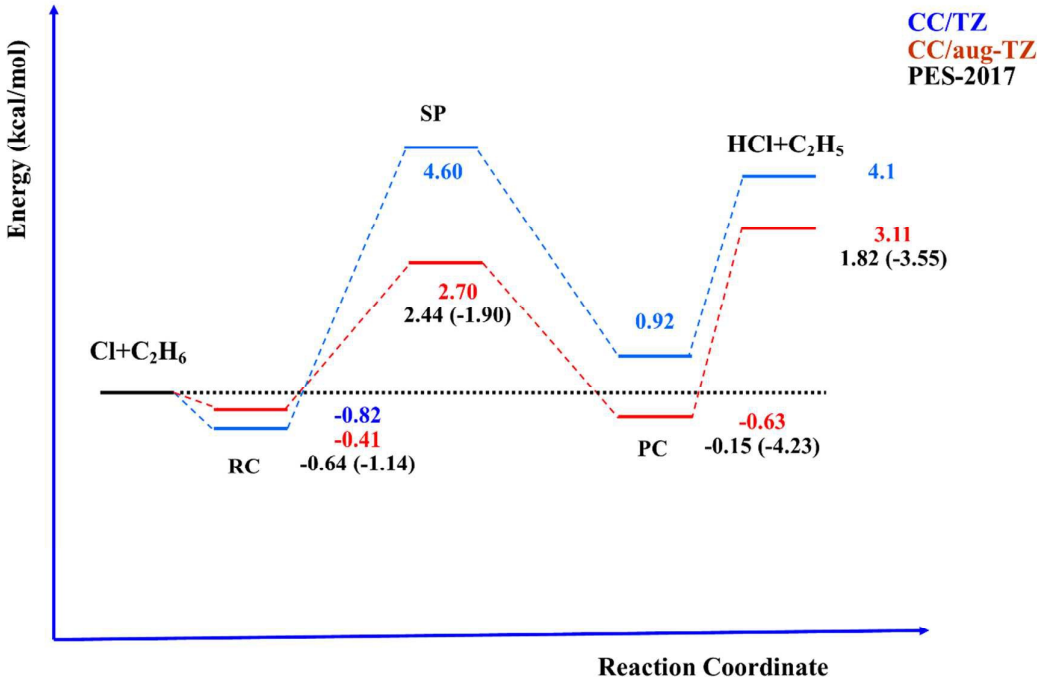

View Article Online
DOI: 10.1039/C7CP07592H

Figure 2

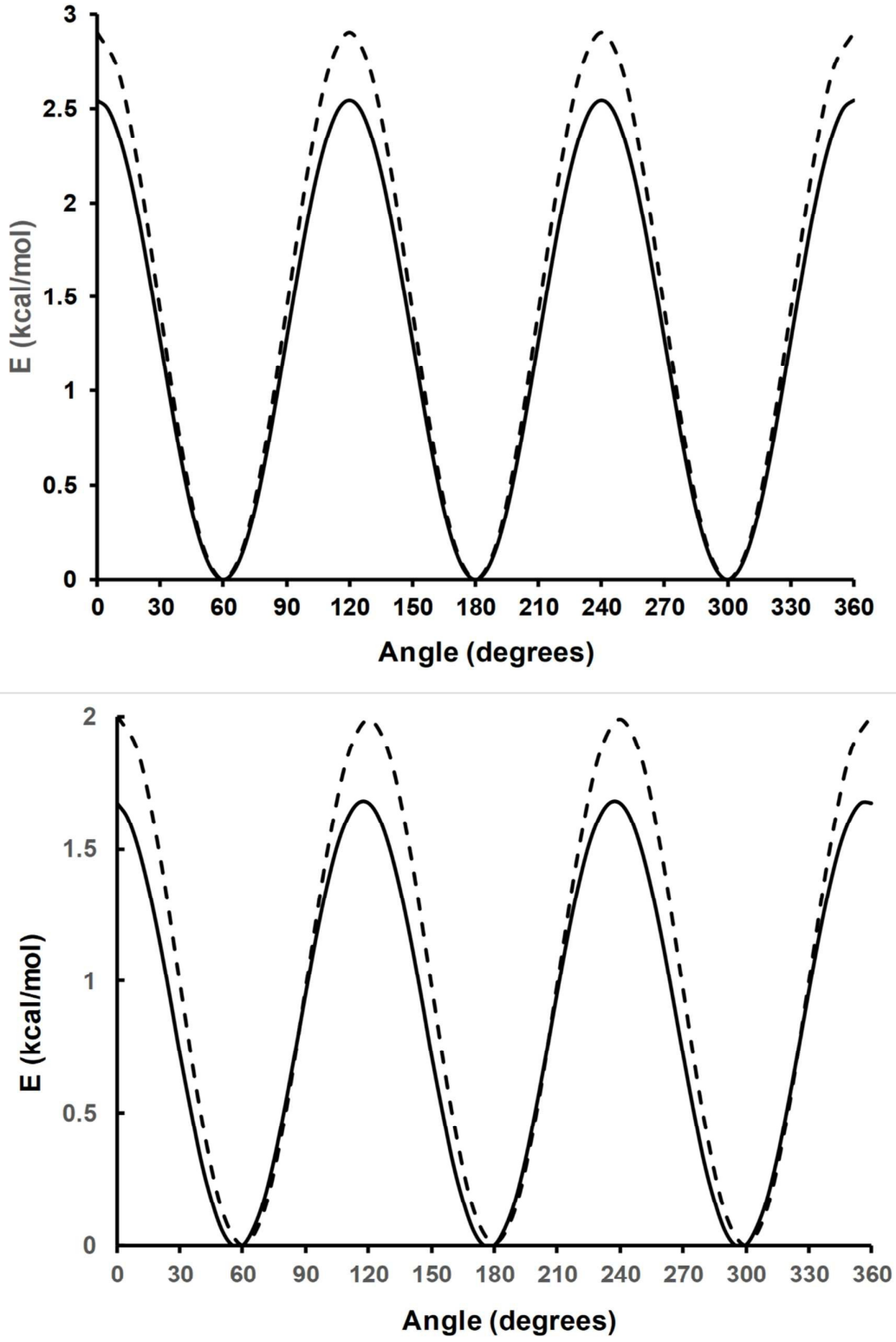

View Article Online
DOI: 10.1039/C7CP07592H

Figure 3

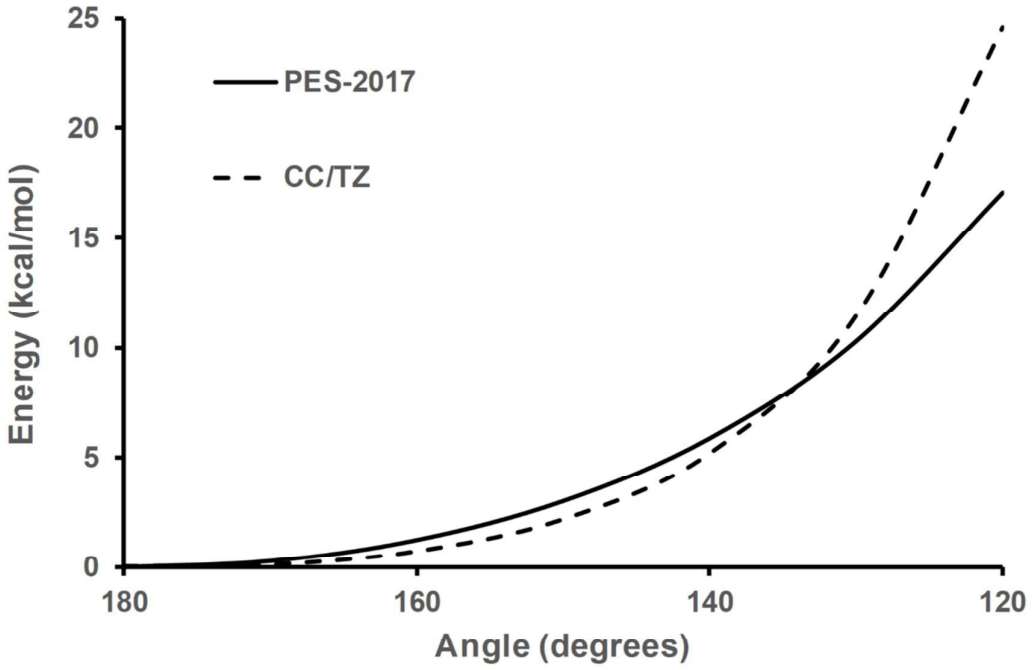

View Article Online
DOI: 10.1039/C7CP07592H

Figure 4

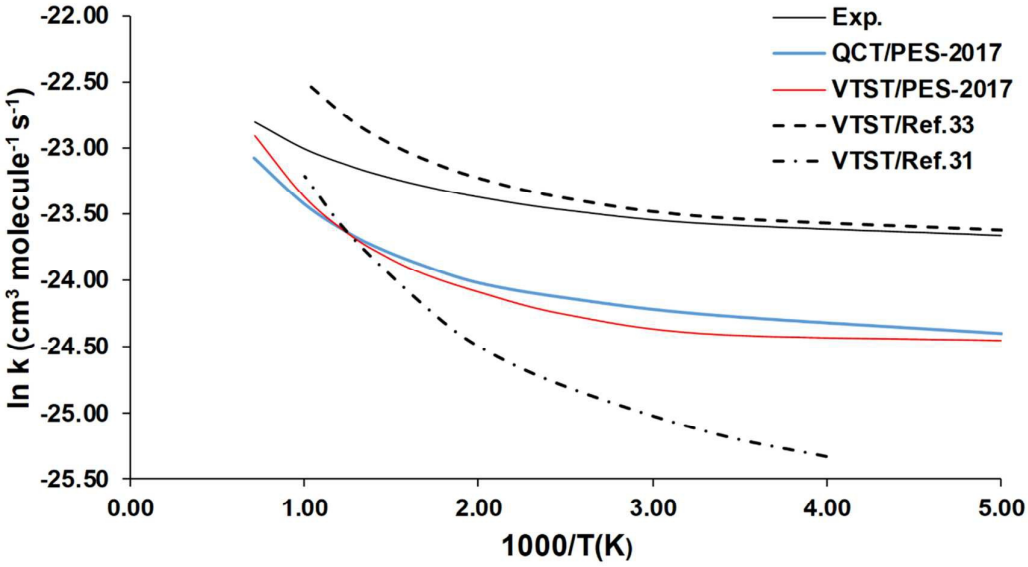

View Article Online
DOI: 10.1039/C7CP07592H

Figure 5